Resonant X-ray Raman scattering for Al, Si and their oxides

J. Szlachetko [a,*], M. Berset [a], J.-Cl. Dousse [a], K. Fennane [a], M. Szlachetko [a], R. Barrett [b], J. Hoszowska [b], A. Kubala-Kukus [c], M. Pajek [c]

[a] *Department of Physics, University of Fribourg, CH-1700 Fribourg, Switzerland*
[b] *European Synchrotron Radiation Facility (ESRF), F-38043 Grenoble, France*
[c] *Swietokrzyska Academy, Institute of Physics, 25-406 Kielce, Poland*

Available online 1 August 2005

Abstract

High-resolution measurements of the resonant X-ray Raman scattering (RRS) of Al and Si and their oxides were performed at the European Synchrotron Radiation Facility (ESRF) in Grenoble, France, using a von Hamos Bragg-type curved crystal spectrometer. To probe the influence of chemical effects on the RRS X-ray spectra, Al_2O_3 and SiO_2 samples were also investigated. The X-ray RRS spectra were measured at different photon beam energies tuned below the K-absorption edge. The measured spectra are compared to results of RRS calculations based on the second-order perturbation theory within the Kramers–Heisenberg approach.

PACS: 32.30.Rj; 32.70.Jz; 32.80.Ys; 31.15.Md

Keywords: X-ray RRS; TXRF; High-resolution XES; Second order perturbation theory

1. Introduction

The application of the total reflection X-ray fluorescence (TXRF) method [1] combined with intense synchrotron X-ray sources offers new possibilities for measuring very low concentrations of light element impurities on the surface of Si wafers. Several experiments [2,3] have shown that the detection limit of Al impurities on Si surface is limited by the presence of the X-ray resonant Raman scattering (RRS). For photon excitation energies tuned below the Si K-absorption edge to avoid the intense Si K fluorescence X-ray line, the RRS structure of Si is indeed overlapping with the Al K X-ray peak. In the analysis of low-resolution TXRF data a precise knowledge of the background profile that is mainly due to the X-ray Raman scattering is therefore crucial. By now, only theoretical predictions [4] were available

* Corresponding author. Tel.: +41 26 300 9080; fax: +41 26 300 9747.
E-mail address: jakub.szlachetko@unifr.ch (J. Szlachetko).

to determine the shape of the RRS structure. However, the assumptions made in these calculations and the resulting uncertainties on the theoretical RRS shape diminish substantially the sensitivity of the TXRF method.

2. Experiment

The RRS X-ray spectra of metallic Al, polycrystalline Si and amorphous Al_2O_3 and SiO_2 samples were measured at the ESRF beamline ID21 by means of high-resolution X-ray spectroscopy, using a von Hamos Bragg-type curved crystal spectrometer [5]. As the Bragg angle domain covered by this instrument extends from 24.4° to 61.1°, for the observation of the 1400–1800 eV X-ray spectra of interest the spectrometer was equipped with an Ammonium Dihydrogen Phosphate ADP (1 0 1) crystal ($2d = 10.642$ Å). The diffracted X-rays were recorded with a 26.8 mm long and 8 mm high position-sensitive back illuminated CCD (Charge Coupled Device) detector consisting of 1340 columns and 400 rows with a pixel size of $20 \times 20\ \mu m^2$. At ID21 the spectrometer was installed downstream of the Scanning Transmission X-ray Microscope (STXM) chamber to which it was connected through a ~200 cm long evacuated pipe.

The X-ray beam was monochromatized by means of two 20 Å Ni/B4C multilayers. Residual higher energy photons were suppressed with a Ni mirror. Thanks to this monochromator 10^{12}–10^{13} incident photons/s were obtained on the targets with an energy resolution of ~6 eV. For all measurements the angle between the incoming beam and the target surface was 20°. 25 mm high × 12 mm wide × 1 mm thick solid targets were used. The specified purity of the targets was better than 99.99% for Al and Si and 97.5% and 99.9%, respectively, for Al_2O_3 and SiO_2.

Data were taken at several excitation energies between 1790 eV and 1900 eV for Si and SiO_2, respectively between 1540 eV and 1600 eV for Al and Al_2O_3. For illustration, the Si and SiO_2, respectively Al and Al_2O_3, RRS spectra are shown in Figs. 1 and 2 for three different excitation energies. The beam energy calibration was determined from measurements of the K-absorption edges of

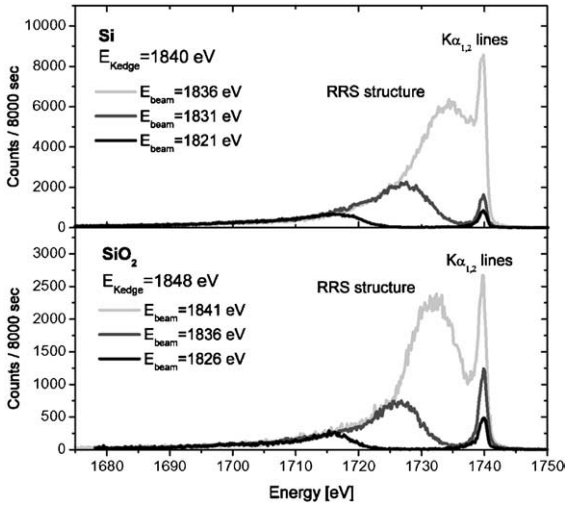

Fig. 1. High-resolution RRS spectra of Si and SiO_2 measured for different excitation energies.

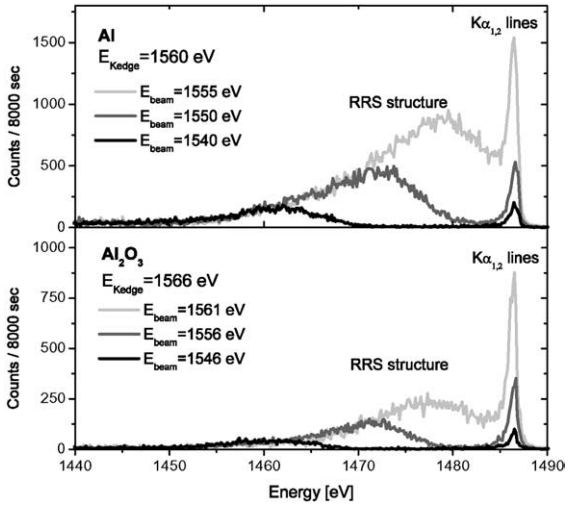

Fig. 2. High-resolution RRS spectra of Al and Al_2O_3 measured for different excitation energies.

Si, SiO_2, Al and Al_2O_3. For each target the intensities of the different spectra were normalized off-line for the number of incident photons and acquisition time and corrected for the beam intensity profile (in the von Hamos slit-geometry, different regions of the crystal surface view different parts of the target so that the shape of the measured spectrum is slightly affected by the spatial

distribution of the beam intensity). The energy calibration of the crystal spectrometer was deduced from measurements of the $K\alpha_{1,2}$ X-ray lines of Al and Si. The same measurements were employed to determine the instrumental broadening of the spectrometer.

3. Results and interpretation

In order to better understand the structures of the measured RRS X-ray spectra, calculations of the resonant Raman scattering around the K-absorption edge with a 2p vacancy in the final state were performed, using the second-order perturbation theory based on the Kramers–Heisenberg formula [6–8]. A more detailed description of these calculations can be found in [9]. An example of a theoretical RRS shape calculated within this model is shown in Fig. 3(a). For comparison with experimental data the theoretical RRS spectra were convoluted with the Gaussian instrumental response of the spectrometer ($\sigma \cong 0.5$ eV) and corrected for the beam energy profile, assuming for the latter a Gaussian shape with a full width at half maximum of $\sim$6 eV.

As an example, the Si RRS spectrum observed at an excitation energy of 1821 eV is compared with the corresponding convoluted theoretical spectrum (thick solid line) in Fig. 3(b). The two thin solid lines whose maxima lie around 1718 eV correspond to the RRS profiles computed for a L_2 or L_3 vacancy in the final state. As shown, the theoretical RRS shape is in good agreement with the experimental data. The $K\alpha_{1,2}$ fluorescence lines which are also visible in Fig. 3(b) are mostly due to the high-energy tail of the beam energy distribution. The two lines were fitted each with a single Voigt profile. Calculations performed for a perfectly monochromatic beam have shown that the centroid positions, shapes and linewidths of the $K\alpha_{1,2}$ transitions are slightly varying when the beam energy is tuned by ± 5 eV around the K-edge [9]. The small differences observed in Fig. 3(b) between the measured and fitted $K\alpha_{1,2}$ lines are probably due to this effect as a consequence of the finite beam energy resolution. The intensity excess found in the low-energy tails of the $K\alpha_{1,2}$ lines corresponds to the excitation of K-shell electrons into the M-shell and quasi-simultaneous filling of the 1s holes by $L_{2,3}$ electrons.

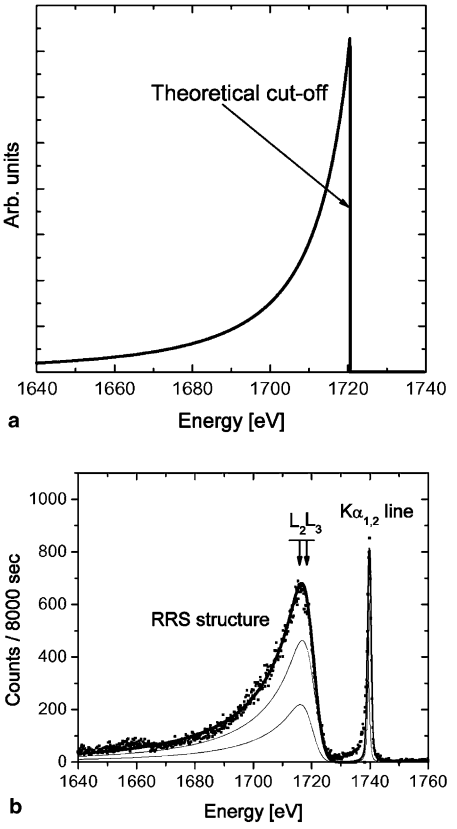

Fig. 3. (a) Theoretical shape of the RRS structure of Si for a beam energy of 1821 eV. The cut-off energy is given by: $\omega_{\text{cut-off}} = \omega_{\text{beam}} - \omega_{\text{L}}$, where ω_{L} stands for the average binding energy of the $L_{2,3}$ subshells. (b) High-resolution RRS spectrum of Si for an excitation energy of 1821 eV. The dots correspond to the experimental data, the thick solid line to the theoretical shape obtained from the sum of the two RRS profiles (thin solid lines) discussed in the text.

An improved analysis of the measured RRS spectra, that needs further calculations to describe the details of the observed features and to determine the influence of the chemical effects on the RRS spectra, will be performed. On the other hand, the measured RRS spectra of Si will be compared to the calculations of Gavrila [4], because the latter have been extensively used to determine the RRS background in low-resolution TXRF spectra.

Acknowledgements

The authors would like to thank Dr. R. Tucoulou and his collaborators of the beam-line ID21 for their excellent support during the experiment. This work was supported by the Swiss National Science Foundation and by the ESRF.

References

[1] R. Klockenkämper, Total Reflection X-ray Fluorescence Analysis, Wiley, New York, 1997.
[2] K. Baur, J. Kerner, S. Brennan, A. Singh, P. Pianetta, J. Appl. Phys. 88 (2000) 4624.
[3] K. Baur, S. Brennan, B. Burrow, D. Werho, P. Pianetta, Spectrochem. Acta B 56 (2001) 2049.
[4] M. Gavrila, Rev. Roum. Phys. 19 (1974) 473.
[5] J. Hoszowska, J.-Cl. Dousse, J. Kern, Ch. Rhême, Nucl. Instr. Meth. Phys. Res. A 376 (1996) 129.
[6] T. Åberg, in: B. Crasemann (Ed.), Atomic Inner-Shell Physics, Plenum Press, New York, 1985, p. 419.
[7] F. Gel'mukhanov, H. Agren, Phys. Rep. 312 (1999) 87.
[8] A. Kotani, S. Shin, Rev. Mod. Phys. 73 (2001) 203.
[9] J. Tulkki, T. Åberg, J. Phys. B 15 (1982) L435.